Process Safety and Environmental Protection 177 (2023) 29–41

Contents lists available at ScienceDirect

Process Safety and Environmental Protection

journal homepage: www.journals.elsevier.com/process-safety-and-environmental-protection

A study on the impact of fuel injection parameters and boost pressure on combustion characteristics in a diesel engine using alcohol/diesel blends

Mustafa Vargün [a,*], Ahmet Necati Özsezen [b,c], Hüseyin Botsalı [a], Cenk Sayın [a]

[a] Department of Mechanical Engineering, Technology Faculty, Marmara University, 34722 Istanbul, Turkey
[b] Department of Automotive Engineering, Technology Faculty, Kocaeli University, 41001 Izmit, Turkey
[c] Alternative Fuels R&D Center, AYARGEM, Kocaeli University, 41001 Izmit, Turkey

ARTICLE INFO

Keywords:
Biofuels
Diesel engine
Engine parameters
FEA
Combustion
Exhaust emissions

ABSTRACT

Engine researchers focused on alcohol fuels since the invention of diesel engines in the 1900s, and the rise in petrochemical costs in the 1970s triggered this concern. This study investigates the impacts of the injection start timing, pilot injection application, and boost air pressure increase, on combustion and exhaust emissions in a common rail diesel engine fueled with ethanol/butan-2-ol/diesel blends. The lowest combustion noise was obtained in the pilot injection application as 83.8 dB in E15B3. The results indicated that the peak point of cylinder gas pressure rose by more than 5 % in the application of pilot fuel injection and advanced injection timing, compared to conventional engine operating conditions. However, maximum CO_2 and NO_x were seen in the pilot injection application using FBDF as 5.7 % and 670 ppm, respectively. As alcohol rate increases in fuel blends, the average 1.3 °CA in the ignition delay period was increased, while the total combustion period was shortened more than 6 °CA. This result shows that the combustion reactions of alcohol/diesel fuels occur faster than pure diesel. However, the variation in the ignition delay and total combustion periods of the test fuels considerably reduced with pilot fuel injection application. These results indicates that pilot fuel injection may be applied very controlled according to changing engine conditions. It was calculated in statistical analysis that except for the coefficient variation of the maximum pressure increase rate, the other coefficient variation values were relatively stable and below 3 %. In addition, it was determined that the results of the finite element analysis are proportional to the pressure values obtained experimentally.

1. Introduction

Demands and consumptions for fossil-based fuels have been increasing at the same speed as the development rates of countries. The exhaust emissions were emitted because of the combustion of these used fossil fuels is harmful to both the environment and human health and lead to cause global warming by causing climate changes. In the world, studies on limiting exhaust emissions and researching alternative fuels of biological origin continue intensively. In this context, researchers have stated that the combustion quality should be improved with development in fuel injection and exhaust emission systems in the vehicle to reduce harmful exhaust gases. Until today, renewable fuels (biodiesel, methanol, ethanol, butanol, etc.), the different injection strategies (injection timing, pilot injection, etc.), and the various intake air pressure (or boost pressure) as the main parameters were utilized to enhance the combustion efficiency in diesel engines by some researchers (Amaral et al., 2016; Ashok et al., 2015; Breuer et al., 2021; De Poures et al., 2023; Gad et al., 2021; Gren et al., 2021; Leach et al., 2020; Nabi et al., 2006; Panoutsou et al., 2021; Saiteja and Ashok, 2021; Xuan et al., 2021).

Diesel engines have high efficiency and durability are used in many areas, such as industry, agriculture, aviation, and railways. A significant drawback of using compression ignition engines is the noise generated by combustion in the cylinder. Controlling noise pollution is one of the critical development parameters in engine design and is regulated by the European Union regulations (Paque, 2003). The characteristics of the fuel used, injection parameters, engine speed, and engine load are critical parameters for controlling the combustion phenomena that cause noise pollution (d'Ambrosio et al., 2022; Dharma et al., 2016; Friedrich and Ortner, 2012; Xin, 2013). As a result of exposure to noise pollution, fundamental problems such as headaches and sleep problems occur.

Studies (Altun et al., 2023; EL-Seesy et al., 2020; Nanthagopal et al.,

* Corresponding author.
E-mail addresses: mustafavargun@gmail.com, mustafa.vargun@marmara.edu.tr (M. Vargün).

https://doi.org/10.1016/j.psep.2023.07.005
Received 13 March 2023; Received in revised form 15 June 2023; Accepted 1 July 2023
Available online 4 July 2023

2020; Ning et al., 2020; Singh and Tsolas, 2023; Yilmaz and Davis, 2022) have shown the usability of low-carbon alcohol fuels in compression ignition engines with three different methods; the injection of alcohol fuels to the intake manifold, the direct injection of alcohol fuels with the developed injection system to the cylinder and mixing the alcohol fuels with the fossil based-diesel fuel with specific proportions. Among these three methods, the least costly and most usable process is mixing low-carbon alcohol fuel with diesel fuel in specific proportions. In addition, since ethanol's production from renewable resources and the oxygen content of it, ethanol has a high usability potential by mixing with pure diesel (Lapuerta et al., 2010; Wang et al., 2021). However, because of the molecular structure of low-carbon alcohol fuel, especially ethanol, the amount of water it contains limits the mixing with diesel fuel. A result of the mix of ethanol at a high percentage with diesel causes phase separation (Kumar et al., 2022; Sarathy et al., 2014). Different co-solvent types have been suggested (Lapuerta et al., 2007; Reyes et al., 2009) in the literature to prevent phase separation, it was stated that the most stable (Jin et al., 2019) results in providing long-term homogeneity in ethanol/diesel mixtures are obtained with the use of butanol. In this article, to keep the ethanol-diesel mixtures homogeneous, butan2ol was added to fuel blends.

Recent studies of diesel engine control parameters point to two critical parameters providing optimum combustion and emission values. These control parameters are the fuel injection timing, dual injection implementation and the intake air characteristics. Lee and Kim (2015) investigated the effects of pilot implementation with using wood pyrolysis oil-ethanol-diesel blends in a diesel engine. They revealed that a late injection of the fuels into the cylinder negatively affects the combustion products. In addition, also it was stated that the pilot injection implementation increases the small amounts of hydrocarbon (HC) and carbon monoxide (CO) emissions. In their study, the coefficient of variation (COV) values was less than 3 % at all examined engine loads. Turkcan (2020) investigated the effects on COV and engine performance by using different biodiesel fuels and ethanol-biodiesel-diesel fuel mixtures in a diesel engine. Also, it was stated that the maximum pressure rise rate (MPRR) and the coefficient of variation of maximum cylinder gas pressure (COV_{Pmax}) value were raised due to the increase in alcohol rate in the fuel blends. Previously, Park et al. (2010) studied the two-staged fuel injection strategies in a compression ignition engine with diesel-ethanol blends. Researchers indicated that the ignition delay prolonged since the ethanol ratio increased in the mixture. It was also determined that increasing the injected amount of pilot fuel injection decreased nitrogen oxide (NO_x) emission however HC emissions increased with the ethanol-diesel mixtures. Duan et al. (2021) investigated the impact of injection start time on combustion and exhaust characteristics by using acetone/butanol/ethanol/diesel fuel mixtures in a compression ignition engine. They stated that advanced fuel injection timing improves the maximum cylinder gas pressure and heat release rate. Researchers found an increase in CO and HC emissions with retarded injection timing. Liu et al. (2014) determined the effect of atmospheric pressure on engine performance in a common rail diesel engine. It was observed that the engine brake torque deteriorated with the rise in the oxygen amount ratio in the fuel mixtures, while the increase in the boost pressure improved the engine brake torque. They found a decrease in BSFC values due to increased boost pressure. Shen et al. (2013) studied the impact of intake air pressure in a single cylinder compression ignition engine using gasoline, ethanol, and diesel fuels. They stated that with the increase of boost pressure, a decline in CO and HC were seen. They stated that adding ethanol to diesel prolonged the ignition delay (ID).

As the above studies show, a diesel engine's performance and emission values change considerably according to the intake air properties and fuel spray behaviors. The main purpose of this study is to investigate the effect of inlet air properties and the fuel injection parameters of a compression ignition engine using alcohol/diesel mixtures on combustion characteristics. In a single-cylinder diesel engine using alcohol/diesel fuel blends, the effect of the thermodynamic properties of the inlet air on the combustion characteristics was investigated by increasing the boost air pressure by 10 % and 20 %. While 45 mg/stroke fuel was injected into the cylinder only in the main injection stage under conventional operating conditions, 10 % pilot fuel injection (4.5 mg) and 90 % main fuel injection (40.5 mg) was applied to determine the impact of pilot injection. Moreover, the effects of advancing and retarding of the start of the fuel spray timing on combustion values were observed. In addition, the compression ignition engine piston used in the study was modeled using the Solid Works program and FEA (finite element analysis) was performed in the ANSYS Workbench program to examine the stress distribution formed by the pressure on the piston.

2. Experimental apparatus and procedure

2.1. Fuel blends preparation

Pure diesel fuel used in experiments was supplied from a national petrol station, a reference diesel fuel conforming to EN95 fuel standards. In addition, J.T. Baker ethanol that has more than 95 % purity was used to mix with pure fossil diesel. Moreover, Merch brand 2-butanol with a purity of 95 % and above was mixed to the blends related to ratio of ethanol in the blends by volume to keep fuel blends more homogeneous. Some characteristics of used test fuels in the experiments are given in Table 1.

In this study, the fossil-based diesel fuel is called FBDF. Blends are named according to the amount of alcohol in the fuel mixture. The E5B1 includes 5 % ethanol + 94 % FBDF and also 20 % of ethanol rate butan2ol (v/v), while the E15B3 includes 15 % ethanol + 82 % FBDF and also 20 % of ethanol rate butan2ol (v/v). The elemental properties of FBDF, E5B1 and E15B3 are given in Table 2.

Ethanol-diesel fuel blends cannot mix homogeneously especially at low ambient temperatures due to density difference; hence a layer occurs between ethanol and diesel fuel. To prevent phase separation and improve engine durability, it was suggested to use solvents or up to 15 % ethanol-diesel fuel mixtures in compression ignition engines. Studies in the literature showed that use of butanol as solvent for ethanol-diesel mixtures is better, compared to other solvents, preventing phase

Table 1
Test fuels properties.

Properties	FBDF (≈$C_{12}H_{24}$)	Ethanol (C_2H_5OH)	2-Butanol (C_4H_9OH)	E5B1	E15B3
Purity	-	≥ 0.99	≥ 0.99	-	-
Molecular Weight (g/mol)	≈ 170	46.07	74.12	162.84	148.53
Latent heat of vaporization (kJ/kg) (Chickos and Acree, 2003)	≈ 256	920	670	293.34	368.02
Density (kg/m^3)	820–845	790	805	817	815.05
Viscosity (mm^2/sec, 40 °C)	2.0–4.5	1.13	3.1	1.96	1.9
Lower Heating Value (MJ/kg)	42.6	26.7	34.4	41.72	39.96
Boiling Point (°C)	160	78	102	-	-
Melting Point (°C)	-9.6	-114.5	-115	-	-
Flash Point (°C)	≥ 55	12	20,5	-	-
Water Content (%)	0,020	≤ 0.2	≤ 0.2	-	-
Cetane Number (Satgé De Caro et al., 2001)	≥ 51	8	15	48.5	43.47
Auto-ignition Temperature (°C)	≈ 210	361	405	-	-

Table 2
Elemental characteristics of FBDF, E5B1 and E15B3.

Some Fuel Properties	FBDF	E5B1	E15B3
FBDF, vol%	100	94	82
Ethanol, vol%	-	5	15
2-Butanol, vol%	-	1	3
C % (v/v)	85.71	85.13	83.82
H % (v/v)	14.29	14.26	14.22
O % (v/v)	-	0.61	1.96

separation due to its chemical properties (Han et al., 2020; Hansen et al., 2005; Huang et al., 2009; Satgé De Caro et al., 2001).

The study observed phase separation before and after addition of 2-butanol to fuel blends. With no addition of 2-butanol, the prepared fuel mixtures separated each other in a short period of about 30 min and became two-layered. On the other hand, observations made after adding sec-butanol to the prepared blends, no visible phase separation occurred from the E5B1 blend in more than a month. In contrast, the E15B3 blend remained homogeneous for up to 3 days, and no visible phase separation occurred.

2.2. Test bench

During the engine tests, a John Deere brand diesel engine with a single-cylinder is 4-stroke, supercharged, water-cooled, and common rail fuel injection system was used at a constant engine speed of 1400 rpm and a constant gas pedal position of 50 % (≈ at 50 % engine load). Some characteristics of the test engine are given in Table 3.

The engine test system consists of three main parts. These can be listed as an eddy current dynamometer, fuel injection system, and engine control unit (ECU). Since the sections in the engine test system can work fully integrated, the system can be controlled via ECU maps. Thus, the effect of instantaneous changes in parameters such as injection start time, amount of separated injection, and pressure of rail line can be observed instantly on the engine. In Figs. 1 and 2 D view of the test bench is given.

In the experiments, AVL brand eddy current dynamometer, which can operate in the range of 0–8000 rpm and measure torque up to a maximum of 190 Nm, was used. In addition, on the cylinder head, a pressure sensor model AVL-GU22C is mounted for observation of cylinder gas pressure measurements. In order to control the intake air pressure, the AVL-515X boost pressure controller was used, and thus the intake air pressure was increased by 10 % and 20 % compared to the standard intake air pressure (240 mbar). The devices used in the experiments and their accuracy rates can be seen in Table 4.

While performing the engine tests, the test environment and measurement methods specified in 8178 were taken as reference, and the engine power measurement was made as recommended in 14,396. Data were taken at each 0.1° CA (crank angle) for the measurement of combustion parameters and for the final values of combustion parameters, the average of 50 cycles were taken. Fuel was injected at an amount of 45 mg/stroke per cycle. In the main stage, the fuel was sprayed in the cylinder with a single injection of 45 mg/stroke at 240 mbar standard intake air pressure (boost pressure) at BTDC (before top dead center) 9.1 °CA. Experiments were carried out in 10 % of boost pressure application and 20 % of boost pressure application, with a single injection of fuel into the cylinder, at the amount of 45 mg/stroke, at BTDC 9.1 °CA, by increasing 10 % boost pressure and 20 % boost pressure respectively, compared to the original intake air pressure. To observe the impacts of the start of injection (SOI), according to the main injection application (at BTDC 9.1 °CA), the SOI was advanced 2 °CA from the TDC (at BTDC 11.1 °CA) and approached by 2 °CA to the TDC (top dead center) (at BTDC 7.1 °CA), with a single injection of fuel into the cylinder at the amount of 45 mg/stroke was sent at 240 mbar standard intake air pressure. In addition, 10 % (4.5 mg at BTDC 14.7 °CA) and 90 % (40.5 mg at BTDC 9.1 °CA) of the fuel were injected into the cylinder during the 10 % pilot fuel injection implementation under 240 mbar standard intake air pressure. The variations in the injection currents for all the injection implementations are given in Fig. 2. In addition, the experimental parameters are given in Table 5.

Table 3
Specification of engine used in experiment.

Engine Type	Single Cylinder – 4 stroke
Fuel System	Common Rail Direct Injection – 1800 bar
Cylinder Volume	1205 cm^3
Valves	3 (2 intake – 1 exhaust) – (OHV)
Max. Cylinder Pressure	190 bar
Max. Engine Speed	2500 rpm
Max. Power	50 kW
Max. Torque	160 Nm
Bore	106.5 mm
Stroke	127 mm
Compression Ratio	16.14

In order to get more accurate results in the experiments and to ensure the engine's stable operation, the engine oil temperature was held up until 90 °C, and then the data were collected. In the experiment test, the intake air temperature, fuel temperature, and cooling water temperature were fixed constant at 25 °C, 20 °C, and 70 °C, respectively. During engine tests, the IMEP, maximum cylinder gas pressure (P_{max}), the MPRR, the CN, the ID, the DOC, NO_x, and CO_2 emission values for each fuel type observed, and coefficient of variation of indicated mean effective pressure (COV_{IMEP}), the COV_{Pmax}, coefficient of variation of combustion noise (COV_{CN}) and coefficient of variation of maximum pressure rise rate (COV_{MPRR}) values were calculated. The obtained results have been compared with FBDF results.

2.3. Calculation of mass fraction burned

The standard zero-dimensional model of the Wiebe function used in engine improvement studies and in determining the combustion phases in the cylinder is as a reference for this study (Liu and Dumitrescu, 2019). This way, combustion stages such as the start of the combustion (SOC), mass fraction burned of fuel, and the end of the combustion (EOC) were examined. The standard zero-dimensional Wiebe function is given in Eq. (1).

$$MFB = \left\{1 - \exp\left(-a\left(\frac{\theta - \theta_0}{\Delta\theta}\right)^{m+1}\right)\right\} \quad (1)$$

Where MFB is the burned mass fraction, θ is the instantaneous crankshaft angle, θ_0 is the crank angle at the start of the combustion, and Δθ is the period from SOC to EOC, and also called as the combustion duration. In addition, m refers the form factor as a constant value and influences the formation of the curve in the combustion process, while a is used as an efficiency factor to control the combustion period processes.

2.4. Calculation of standard deviation and coefficient of variation

In this study, 50 cycles were averaged for each test case. The result of each parameter measured in the experiments was taken as the absolute average value of all the measured values. Eq. (2) was used to calculate the mean of the measured values. Standard deviation of the measured parameters were calculated to determine the uncertainty of the experiments. The standard deviation (SD) was calculated using the formula in Eq. (3).

$$\overline{X} = \frac{\sum_{i=1}^{n} X_i}{n} \quad (2)$$

Where, $\overline{X}$ shows average of measured values, X_i shows measured value i.

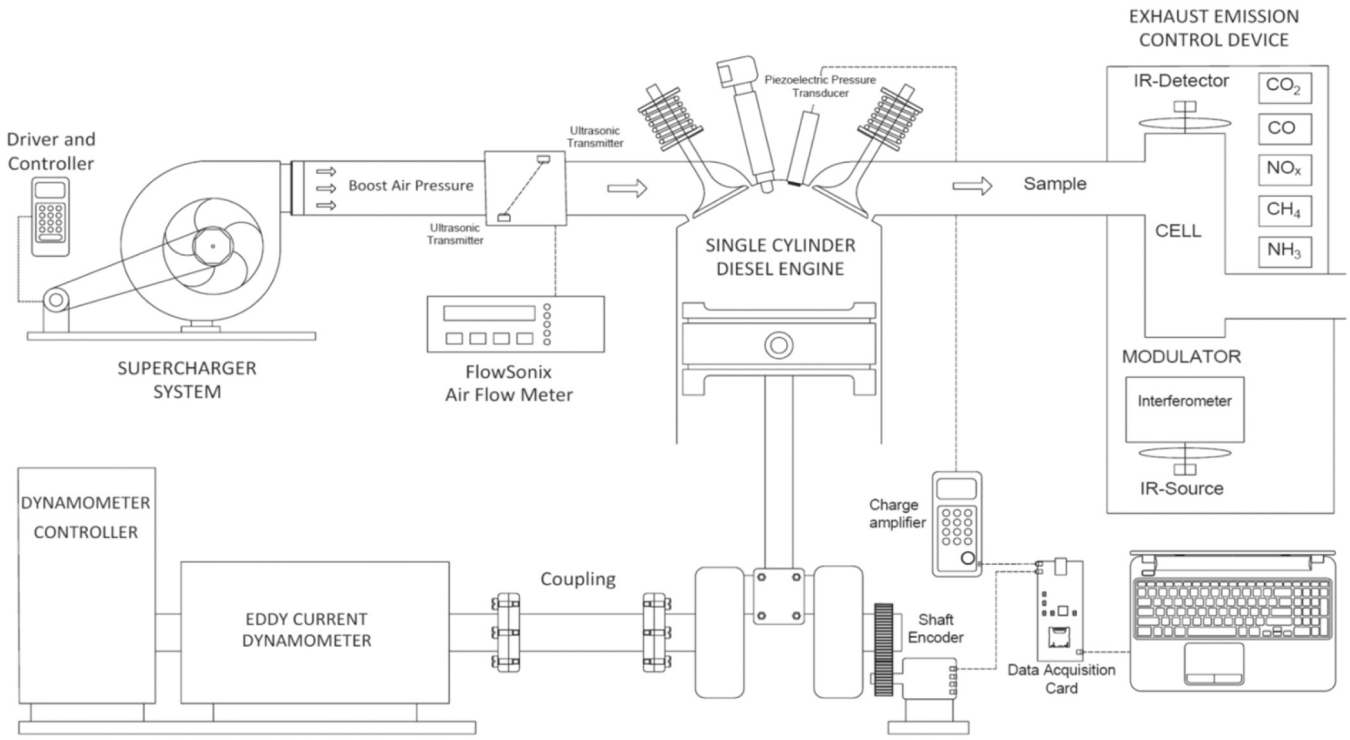

Fig. 1. 2D view of the test bench.

value in the loop, n is number of samples.

$$SD = \sqrt{\frac{\sum_{i=1}^{n}(X_i - \overline{X})^2}{n-1}} \tag{3}$$

In the experiments, COV analysis was carried out to specify whether the engine was stable or not. It can be said that if COV values are lower than 3 %, the engine runs quite stable. COV value of less than 3–5 % is considered an indication of good drivability (Biswas et al., 2021). However, COV values should not be more than 10 % for normal engine runs. In addition, the COV values are used to determine the cycle difference of the combustion in the cylinder (Liu et al., 2022). By taking the average of 50 cycles, COV analysis was performed for IMEP, the maximum cylinder gas pressure, the maximum pressure rise rate, combustion noise parameters. Eq.4 was used to calculate the coefficient of variation values.

$$COV = \frac{SD}{\overline{X}} x100 \tag{4}$$

2.5. Calculation of combustion noise

The pressure data in the cylinder were collected using the AVL IndiCom software over the pressure sensor placed in the cylinder. Combustion noise was calculated using AVL IndiCom software based on the pressure data inside the cylinder. A transformation to the third-octave spectrum follows the normal Fourier transformation. Using spectral lines, it defines the average data level in dB in the third-octave band. Then the pressure value is filtered to calculate the root mean square pressure (P_{rms}) and the final noise level is obtained by comparing the P_{rms} with the reference sound level (d'd'd'Ambrosio et al., 2019). For calculation of combustion noise, Eq.5.was used as given below.

$$Noise \quad (dB) = 20 * \log_{10}\left(\frac{P_{rms}}{20\mu Pa}\right) \tag{5}$$

2.6. Numerical Study

In this part, finite element analysis is carried out in order to calculate the stresses acting on the diesel engine piston using the pressure values obtained in the experimental phase of the study. First, a 3D solid model of the piston was obtained using SOLIDWORKS software. Later, this model was transferred to ANSYS Workbench in STEP file format to perform static structural analysis. A tetrahedral element is used to create the finite element mesh. In the mesh convergence process given in Table 6, von Mises stress was taken into account and the point where the difference decreased to 0.6 % was accepted as the appropriate mesh structure. The mesh model with 353,604 elements and 512,957 nodes is shown in Fig. 3. The material properties required for static structural analysis are defined as Young's modulus of 75 GPa and Poisson's ratio of 0.33 (Koutsakis and Ghandhi, 2022). The fixtures are defined from the piston pin holes as cylindrical supports. In-cylinder pressure values obtained in the experimental part were applied from the piston top and analyses were carried out.

3. Result and discussion

3.1. Indicated mean effective pressure (IMEP)

IMEP is an indicator of engine torque depending on the cylinder gas pressure, and it is a fundamental parameter to determine engine efficiency (Ge et al., 2022). Fig. 4 shows change in IMEP under different control parameters. As seen in Fig. 4, the rise in the alcohol rate in the mixtures under the same test conditions caused a decrease in IMEP. Among the all test conditions, the highest IMEP was achieved in FBDF as 7.8 bar at 10 % pilot fuel injection implementation. In the main fuel injection implementation, the highest IMEP value was obtained as 7.03 bar by using FBDF, while there was a decline in IMEP with E5B1 and E15B3 fuels and was calculated as 6.74 bar and 6.6 bar, respectively.

All fuels compared to each other in the main test applications, it was determined that the + 2 °CA injection application caused a slight

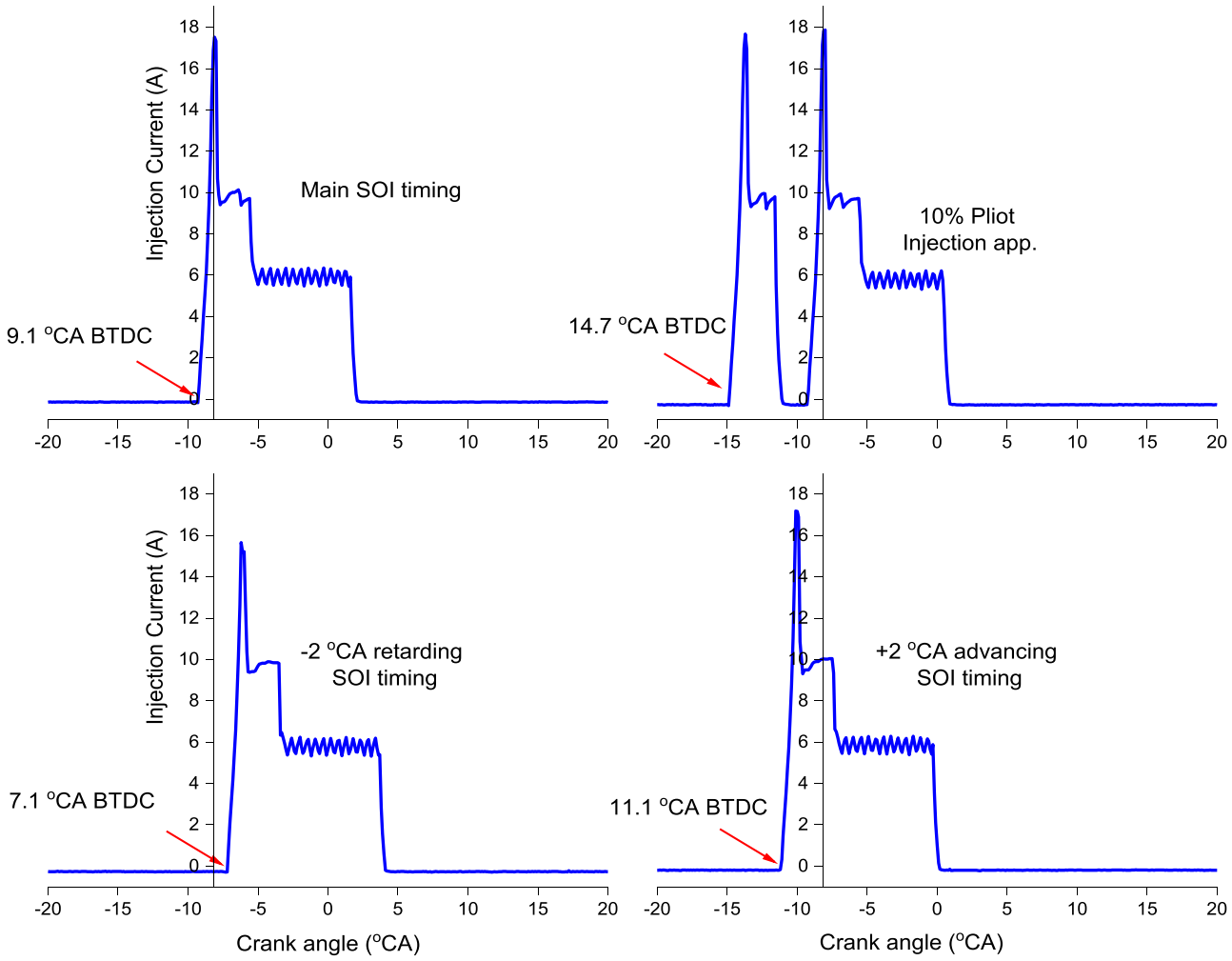

Fig. 2. The variations in the injection currents for all the fuel injection applications.

Table 4
Accuracy of the test devices.

Measurement	Device	Accuracy
Torque	HBM Torque Flange	± 0.1 %
Engine Speed	AVL Encoder	≤ ± 0.1CA
Test Cell Humidity and Temperature	Vaisala – HMT 330	± 1 % RH, ± 0.2 °C
In-cylinder Pressure	AVL-GU22C	0.05CA
Injection timing	Angle Encoder	± 0.1CA
Engine Coolant & Oil Conditioning	AVL-577	± 1 K
Fuel Consumption	AVL-735	< 0.15 %
NO_x	AVL AMA i60	≤ ± 1 %
Temperature Sensors	PT100 (K Type)	≤ ± 1 %

increase in IMEP, while the − 2 °CA injection application caused a decrease in IMEP. Compared to the IMEP obtained in the main application with FBDF, the use of 10 % boost application, 20 % boost application, 10 % pilot fuel injection application and + 2 °CA injection

Table 6
Mesh convergence of mean value.

Element Number	Node Number	von Mises Stress (MPa)
38,459	61,062	89.461
75,267	115,198	90.242
183,265	270,741	94.557
353,604	512,957	94.563

Table 5
The experimental parameters.

	Test 1	Test 2	Test 3	Test 4	Test 5	Test 6
Engine speed	1400 rpm	1400 rpm	1400 rpm	1400 rpm	1400 rpm	1400 rpm
Fuel types	FBDF, E5B1, E15B3	FBDF, E5B1, E15B3	FBDF, E5B1, E15B3	FBDF, E5B1, E15B3	FBDF, E5B1, E15B3	FBDF, E5B1, E15B3
Engine load	50 %	50 %	50 %	50 %	50 %	50 %
Engine coolant temperature	70 °C	70 °C	70 °C	70 °C	70 °C	70 °C
Engine oil temperature	90 °C	90 °C	90 °C	90 °C	90 °C	90 °C
Air temperature	25 °C	25 °C	25 °C	25 °C	25 °C	25 °C
Air intake pressure	24 kPa	26.4 kPa	28.8 kPa	24 kPa	24 kPa	24 kPa
Amount of total injected fuel	45 mg/stroke	45 mg/stroke	45 mg/stroke	45 mg/stroke	45 mg/stroke	4.5 + 40.5 mg/stroke
Start of main injection	9.1 °CA BTDC	9.1 °CA BTDC	9.1 °CA BTDC	11.1 °CA BTDC	7.1 °CA BTDC	9.1 °CA BTDC
Start of pilot injection	-	-	-	-	-	14.7 °CA BTDC

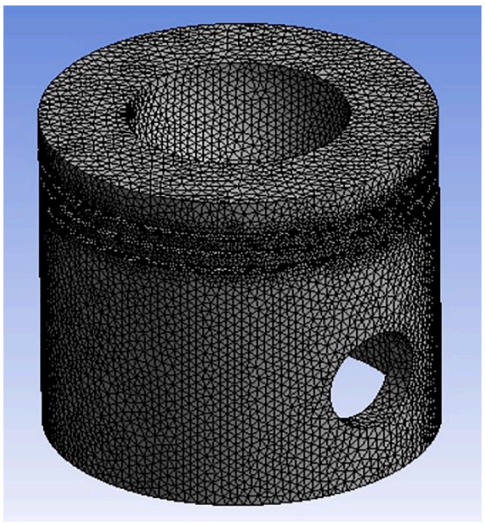

Fig. 3. FEA element mesh model of piston.

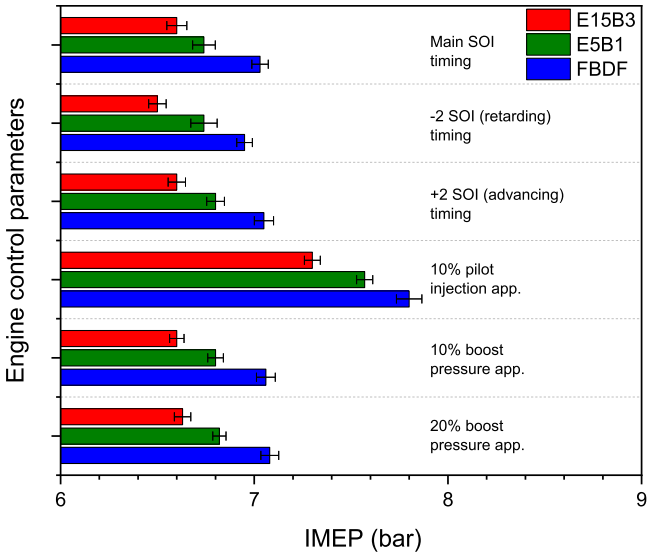

Fig. 4. Change in IMEP under different engine parameters.

application caused a slight improvement in IMEP, while worsening in IMEP was detected in − 2 °CA injection applications. The maximum IMEP values of E5B1 and E15B3 were observed as 7.57 bar and 7.3 bar, respectively, in 10 % of the pilot fuel injection application.

3.2. Cylinder gas pressure (CGP)

Fig. 5 shows change in CGP under different control parameters. The adjacent-averaging filter method was used to obtain a smooth CGP trace. In all the test conditions, the highest P_{max} was obtained with E5B1 at the + 2 °CA injection timing and 84.1 bar at ATDC (after top dead center) 7.8 °CA. On the other hand, it was observed that the − 2 °CA fuel injection timing causes a decline in the P_{max} for all fuels. Using the same engine control parameter, the blends rise P_{max} values. In the main fuel injection application, the P_{max} values enhanced with the increased alcohol amount in the blend, and they closed to the TDC (FBDF: 74.5 bar at 9.8 °CA ATDC, E5B1: 76.4 bar at 8.8 °CA ATDC and 80.5 bar at 6 °CA ATDC). Similar results were found by some researchers (Kim et al., 2020; Zhang et al., 2022). It can be explained with oxygen content in the blended fuels that improves and accelerates the combustion.

Compared with the main fuel injection implementation, it was determined that the pilot fuel injection implementation significantly increased P_{max} in all test fuels. In the 10 % pilot implementation, P_{max} was achieved as 80.9 bar for FBDF, 81.7 bar for E5B1 and approximately 81 bar for E15B3. In 10 % increased intake air pressure, it was determined that the blends caused a slight increase in P_{max} values compared to neat FBDF, while P_{max} values were very close to each other in the 20 % increased intake air pressure. Compared to the main fuel injection implementation, it was obtained that intake air pressure applications improved P_{max} values, which was thought to be because of the combustion improvement by taking more oxygen into the cylinder in the boost applications.

3.3. Ignition delay (ID), duration of combustion (DOC), and mass fraction burned of 50 % (MFB50)

ID can be expressed as the time from the injection of fuel into the cylinder to the first ignition of the fuel. Fig. 6 shows change in ID under different control parameters. It was observed that the ID showed an increasing trend with the oxygenated fuel. In the main application, the longest ID was determined as 9.05 °CA as a result of using the fuel type containing at least FBDF fuel, while the ID was obtained as 7.36 °CA in pure FBDF. In the experimental test carried out with the same engine parameter, the rise in alcohol amount in the blend caused the ID to be prolonged in general. This is thought to be due to alcohol fuels have lower cetane number and higher latent heat of vaporization (Cova--Bonillo et al., 2022; Zhao et al., 2022). Among the experimental test, the most extended ID was determined as 9.12 °CA in the + 2 °CA fuel injection application with E15B3. In comparison, the shortest ID was obtained as 7.24 °CA as a result of %20 increased boost pressure with FBDF use. In addition, a slight shortening of the ID was found for FBDF and E15B3 at 20 % increased boost pressure compared to 10 % increased boost pressure. Also, it was seen that taking the fuel injection timing 2 °CA earlier than the main injection time of the fuels with a main injection caused the ID to be prolonged, while approaching the SOI 2 °CA to the TDC caused the ID to shorten. In literature, Guedes et al. (2018) reported similar results. This can be explained with the temperature in the cylinder is lower when the fuels are sent to the early cylinder, and the inside of the cylinder is warmer when the fuels are injected closer to the TDC.

As seen in Fig. 6, the impacts of the engine control parameters and the test fuels on DOC were given. When the test fuels were compared among themselves, DOC tended to decrease as the ratio of ethanol and 2-butanol in the blend fuels increased. When the DOC values calculated in the main application are compared, the fastest combustion event in the cylinder was obtained as 33.55 °CA with the use of E15B3, while the DOC increased by approximately 7 °CA in the use of FBDF, an increase in DOC of more than 2.5 °CA was found with E5B1. It is thought that the DOC shortens with the use of the blends since the oxygen molecules of the blends improve the combustion in the cylinder and provide faster combustion (Chen et al., 2013). For all the test fuels, a 10 % boost increase and a 20 % boost increase compared to the main application are seen to cause a slight shortening of the DOC, while it is thought that this situation is due to the fact that the rise in the intake air pressure allows more air to be received into the cylinder and hence the combustion takes place faster. The shortest DOC was reached for FBDF, E5B1 and E15B3 in the − 2° CA injection applications (39.8 °CA, 35.77 °CA and 32.3 °CA, respectively). Compared to the main application, the 10 % pilot fuel injection implementation caused the DOC to be prolonged for all fuel types. The reason for this situation is thought to be because 10 % of the fuel is injected 5.6 °CA before the main injection with the pilot injection.

Fig. 7 shows the effects of the engine control parameters and the test fuels on the mass fraction burned of 50 % (MFB50). The moment when 50 % of the fuel is burned is accepted as the moment when the energy of the fuel is transferred into heat energy (Bunting et al., 2007). As seen in Fig. 7, in all test conditions, the rise in ethanol and butan2ol fuels rate in the mixture fuels caused the MFB50 point to be achieved in a shorter

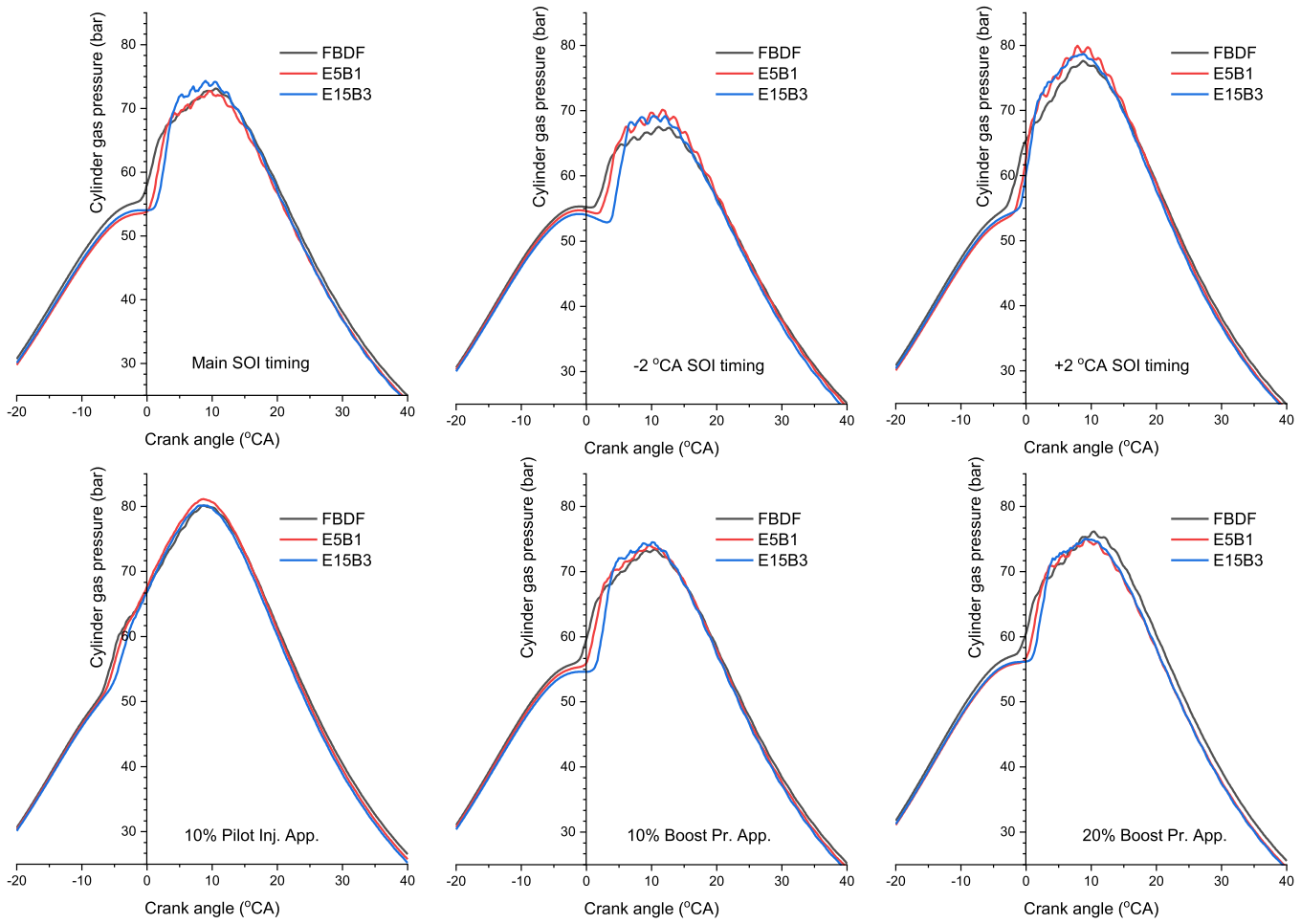

Fig. 5. Change in CGP under different engine parameters.

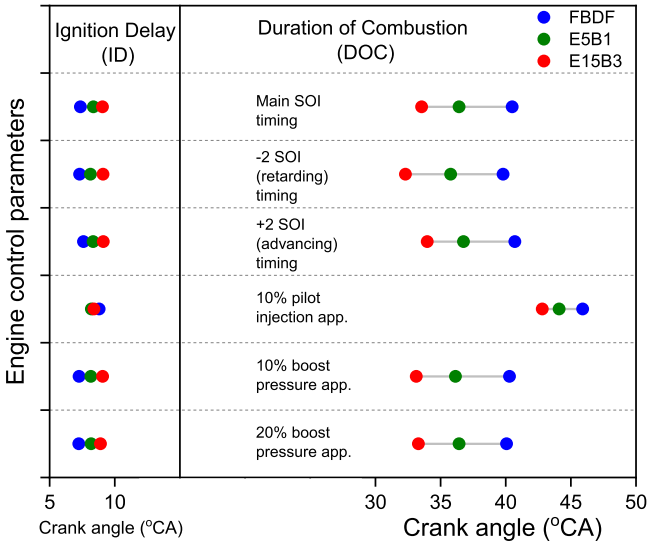

Fig. 6. Change in ID and DOC under different engine parameters.

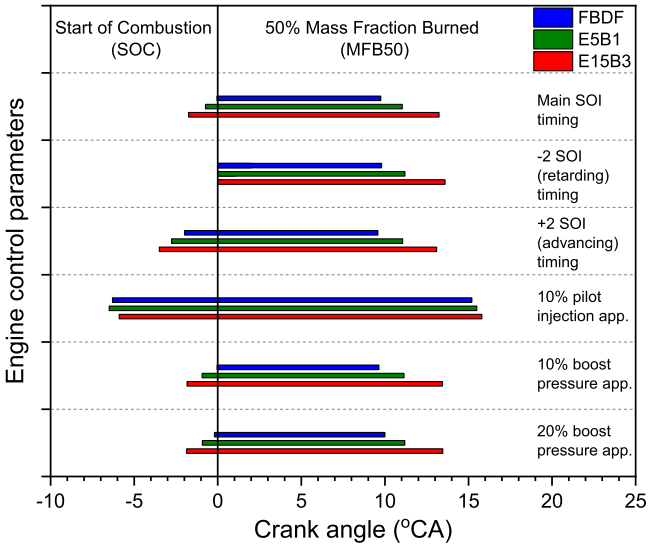

Fig. 7. Change in SOC and MFB50 under different engine parameters.

time. In experiments with the main application, the shortest MFB50 time was 9.75 °CA with E15B3, 11.04 °CA with E5B1, and 13.24 °CA with FBDF. The using blends enabled the chemical energy of the fuel to be converted into heat energy earlier, it is thought that this situation occurs since the oxygen content of ethanol-butan2ol improves the combustion in the cylinder and provides faster combustion. For all the fuel types, 20 % boost pressure application was found to slightly delay the acquisition of MFB50 compared to 10 % boost application. With 10 % pilot implementation, the acquisition of MFB50 was determined as 15.2 °CA in E15B3, while it was observed that it took as long as 0.6 °CA and 0.3 °CA

in the use of FBDF and E5B1 fuel, respectively. In addition, it was determined that the MFB50 duration, which was observed as a result of the main application in FBDF and E15B3, was slightly prolonged in the − 2 °CA injection application, while a shortening trend was observed in the MFB50 period as a result of the + 2 °CA injection application.

3.4. Maximum pressure rise rate (MPRR)

While the pressure rise rate defines the force applied to the piston at each crank angle, higher than 10 bar/°CA causes the engine to knock (Wang et al., 2015). Fig. 8 indicates the impacts of the engine control parameters and the test fuels on MPRR. The highest MPRR value was determined as 13 bar/°CA in + 2 °CA injection application as a result of using E15B3, which is 30 % higher than the MPRR value predicted for a knock-free operation of the engine. Ethanol/2-butanol/diesel blends were shown to cause an overall increase in MPRR. In addition, it was seen that the MPRR rose due to the increase in the ethanol-secbutanol content in the blend fuels. It was observed that there was an 80 % rise in the MPRR of the blended fuels under the main application conditions. The MPRR value of the E5B1 exceeded 10 bar/°CA in only the 20 % increased boost pressure application and reached the value where the engine would tend to knock. It is thought that the reason why the MPRR for the mixture fuels are higher than the MPRR values of the FBDF is due to the sudden pressure increases with the combustion of more fuel together as a result of the prolonged ID since the low cetane number of the ethanol-secbutanol in the blends.

On the other hand, when compared to the main application, a decreasing trend was detected in MPRR values in all the fuel types in the − 2° CA injection implementation, and the MPRR values remained below 10 bar/°CA; the MPRR values were obtained as 5.6 bar/°CA for FBDF, 8.4 bar/°CA for E5B1, and 9 bar/°CA for E15B3. In the 10 % pilot implementation, it is thought that controlled combustion occurs in the cylinder by sending the test fuels as 10 %+ 90 % in two stages, and thus the MPRR value is controlled for each the fuel types. With 10 % pilot fuel injection application, the MPRR values of E5B1 and E15B3 fuels were found to be 4.6 bar/°CA, lower than the MPRR value of FBDF 6.1 bar/°CA.

3.5. Combustion noise (CN)

Fig. 9 shows the impacts of the engine control parameters and the test fuels on CN. As seen in fig, 10 % pilot fuel injection application caused a significant downward trend in CN for all test fuels. The lowest

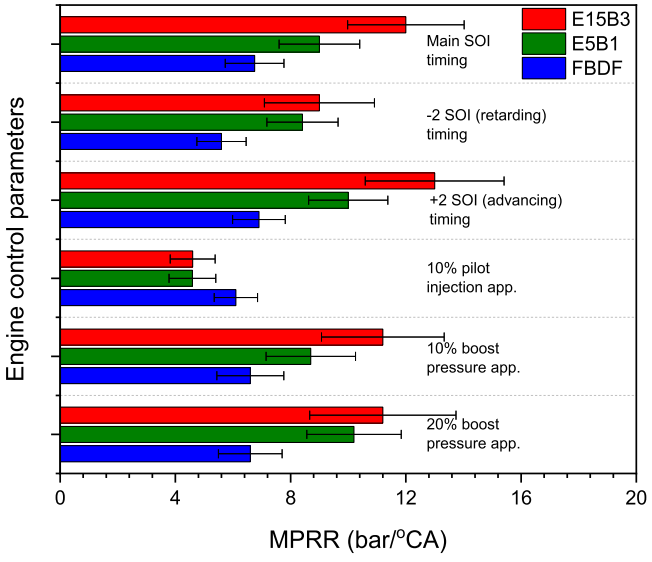

Fig. 8. Change in MPRR under different engine parameters.

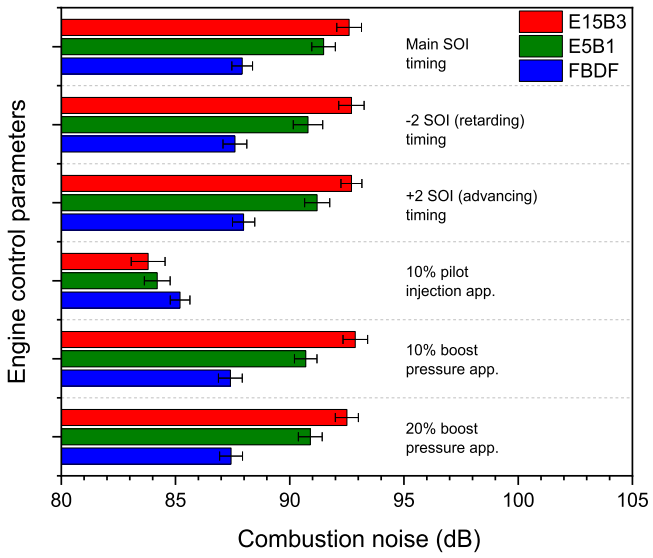

Fig. 9. Change in CN under different engine parameters.

CN for all the fuel types were determined as 85.2 dB for FBDF, 84.2 dB for E5B1 and 83.8 dB for E15B3 with 10 % pilot implementation. It is thought that due to sending the fuels to the cylinder with two separate injections, a controlled combustion is achieved in the cylinder and a decrease in CN is observed due to the control of the pressure increase rate. The CN of FBDF was 87.98 dB with a slight increase in the + 2 °CA injection application compared to the CN value in the main application, while it was measured as 87.6 dB, showing a slight decrease in the − 2 °CA injection application.

At the same time, it was determined that CN showed an increasing trend due to the rise in ethanol-butan2ol ratio in blend fuels compared to FBDF. While the CN value of FBDF was measured as 87.92 dB in the main application, CN increased by approximately 3.5 dB and 4.5 dB in the use of E5B1 and E15B3 respectively in the same application. Since the low cetane number of ethanol-butan2ol, it is thought that CN tends to increase with the use of the mixture fuels, due to the increased MPRR as a result of the effect of prolonged ID. For each test fuels, it was seen that the CN values of 10 % boost and 20 % boost applications are close to each other and lower than the main application.

3.6. Nitrogen oxide (NO_x) emissions

NO_x is an exhaust emission that occurs due to the reaction of oxygen and nitrogen by reaching high temperatures (1800 K and above) in the cylinder. Fig. 10 shows change in NOx emissions under different control parameters. The pilot injection application caused an important rise in NO_x emission and compared to the main fuel injection application, using pilot injection resulted in an increase of NO_x by approximately 40 % for FBDF fuel, more than 10 % for E15B3, and approximately 10 % for E5B1 fuel. With the use of the pilot implementation, the fuels are sent into the cylinder in two stages, and 10 % of the fuel sent in the first injection rises the temperature of the cylinder, and it is thought that an increase in NO_x because 90 % of the fuels are sent in the second injection, providing better combustion, and reaching higher temperatures. Similar results were reported by Liu et al. (2022) for methanol/diesel blends. Retarded SOI timing to TDC by 2 °CA (at 7.1 °CA BTDC) resulted in the lowest NO_x emissions for all the fuel types, with 422 ppm in FBDF fuel, 446 ppm in E5B1, and 443 ppm in E15B3. It is thought that with retarding the injection timing, the time required for the fuels to mix homogeneously with the air and provide a good combustion is shortened, and since a certain part of the fuel is burned after the TDC, it causes lower combustion temperature and leads a reduction in NO_x emissions.

Compared to FBDF, NO_x emission of E15B3 was found to be higher in

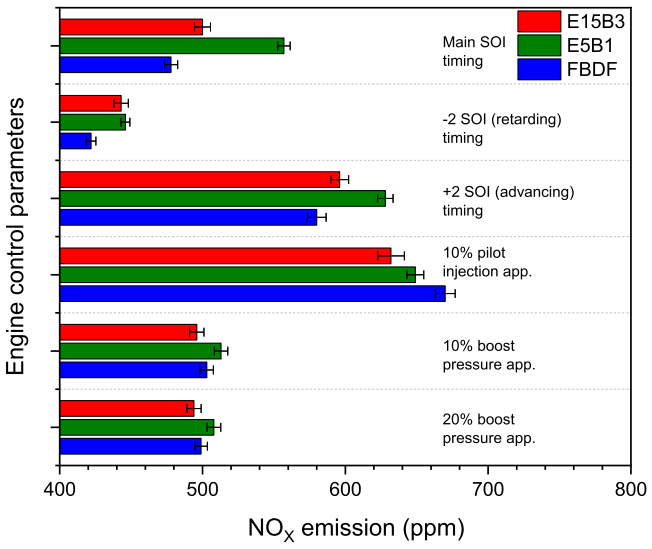

Fig. 10. Change in NO_x under different engine parameters.

main, 10 % boost, 20 % boost, + 2 °CA, and − 2 °CA applications. The main reason for this situation is thought that the oxygen-containing fuel has better combustion in the cylinder. The NO_x values of E15B3 decreased at high level of the boost pressure compared to the main application. Moreover, it was determined that the injection of the fuels into the cylinder at BTDC 11.1 °CA causes an increase in NO_x emissions, compared to the injection of fuels at BTDC 9.1 °CA. Also, Li et al. (2022) stated that advanced SOI timing increases NO_x emission level. The fact that the earlier injection of the fuels into the cylinder causes a rise in NO_x can be expressed by the rise in the temperature of the cylinder together with the improvement of the combustion in the cylinder due to obtaining more time for the fuels to mix homogeneously with the air and burning more fuel BTDC.

3.7. Carbon dioxide (CO_2) emission

CO_2 emission is formed by the reaction of carbon and oxygen as a product of complete combustion. In addition, preventing the release of CO_2 emissions, which is shown as the primary cause of global climate change, is a matter of worldwide importance. Fig. 11 indicates the impacts of the engine control parameters and the test fuels on CO_2. It was determined that 10 % pilot fuel implementation is the cause of the maximum CO_2 emission for each fuels. In 10 % pilot fuel injection, the CO_2 emission values were found to be 5.7 % for FBDF, 5.5 % for E5B1, and 5.34 % for E15B3. In the implementation of main injection, while FBDF caused the maximum CO_2 as 4.94 %, it was determined that the CO_2 emission of E5B1 and E15B3 were equal to each other as 4.82 %. Moreover, in the two-stage fuel injection, an increase in CO_2 was detected since the improvement of the combustion in the cylinder, while it can be defined that the reason for the rise in CO_2 with FBDF compared to the mixed fuels is due to the high C/H ratio.

Compared to the main injection application, the emission of CO_2 by advancing the injection timing (+2 °CA injection application) was found to be more than 5 % for FBDF and E5B1, and less than 5 % for E15B3. It is thought that there is an increase in CO_2 emissions due to the fact that a more homogeneous air-fuel mixture is obtained in the cylinder by taking the injection timing earlier, hence a better combustion event occurs. Moreover, CO_2 emission was measured as 4.94 % with the implementation of main injection in FBDF, while it was measured as 4.9 % and 4.82 % in the 10 % boost application and 20 % boost application, respectively.

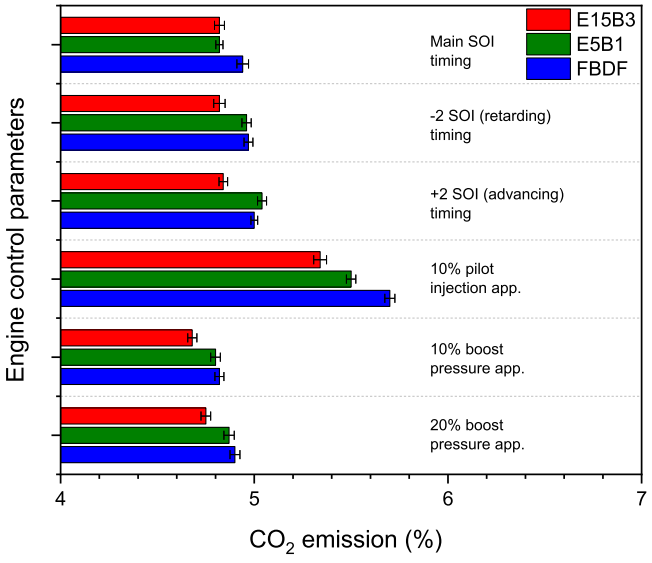

Fig. 11. Change in CO_2 under different engine parameters.

3.8. Coefficient of variation (COV)

Fig. 12 indicates the effects of the engine control parameters and the test fuels on COV_{CN}. The COV_{CN} was found to be less than 1 % under all the test conditions. In all fuel types, the highest COV_{CN} values were obtained in the − 2 °CA injection application. In all the test conditions, the highest COV_{CN} was calculated as 0.77 % in the − 2 °CA injection applications in E15B3, which has the highest alcohol fuel content. Compared to FBDF under the same engine test conditions, it was seen that the increase in the ratio of alcohol fuel ratio in the mixture increased the COV_{CN} value in general. This is thought to be due to the fuel characteristics (such as high oxygen content and low viscosity) that change with the mixing of fuels. In the experiments carried out under the main application, the lowest COV_{CN} value was calculated as 0.51 % in the use of FBDF, while it was calculated as 0.51 % and 0.53 % in the E5B1 and E15B3 under the same test conditions. Considering all the test conditions, it was seen that the COV_{CN} values varied between 0.5 % and 0.77 %, and the change in the CN values turned out to be quite stable.

Fig. 13 shows the effects of the engine control parameters and the test fuels on COV_{IMEP}. As seen in fig., considering the COV_{IMEP} values, the maximum COV_{IMEP} value for FBDF was calculated as 0.84 % in the 10 % pilot implementation, while the minimum COV_{IMEP} was calculated

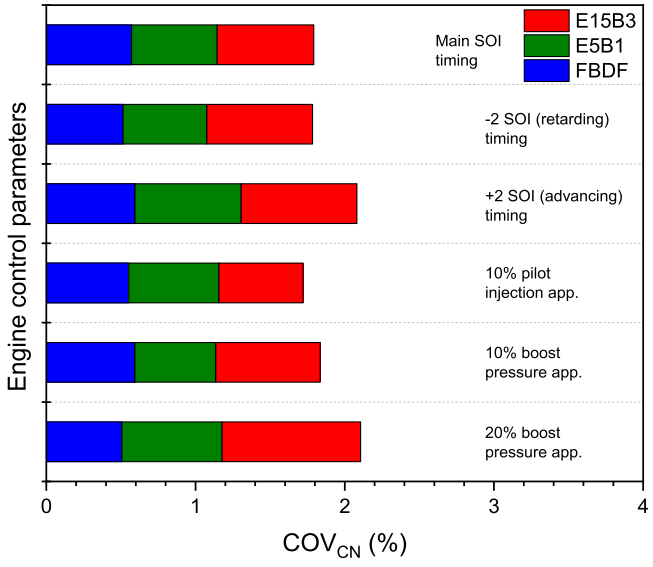

Fig. 12. Change in COV_{CN} under different engine parameters.

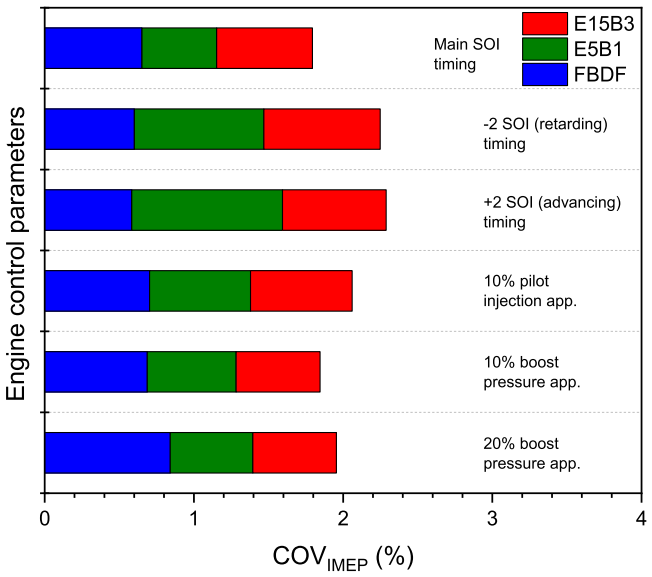

Fig. 13. Change in COV_{IMEP} under different engine parameters.

as 0.58 % in the − 2 °CA injection application. In addition, it was determined that in E5B1 and E15B3 fuels caused an increase in the COV_{IMEP} values compared to FBDF in the main application conditions. In all the test conditions, the maximum COV_{IMEP} was 1.01 % in the − 2 °CA SOI timing with the use of E5B1. This situation is thought to be caused by the lack of a good combustion event due to the fact that there is not enough time for the homogeneous mixing of the fuels as a consequence of the application of the -2^{o} CA fuel injection timing, while it is also thought that a low cetane number and a high latent vaporization heat of alcohol fuels cause a rise in COV_{IMEP}. Compared to the main application, the use of E5B1 and E15B3 fuels in 10 % boost application reduced COV_{IMEP} by more than 20 %. This can be explained by a better combustion event occurs because the rise in the intake air pressure escalates the amount of air taken into the cylinder.

Fig. 14 illustrates the impacts of the engine control parameters and the test fuels on COV_{Pmax}. It was found that COV_{Pmax} decreased in 10 % boost application, 20 % boost application, 10 % pilot fuel application, and the + 2 °CA injection implementation compared to the main injection implementation, while delaying the injection start timing (−2 °CA injection applications) caused a slight increase in COV_{Pmax} for all test fuels. When consider all the test conditions, the maximum COV_{Pmax} was 2.33 % with approximating the SOI timing to the TDC in the use of E15B3 containing maximum alcohol amount, while taking the injection timing earlier in the same fuel type caused the COV_{Pmax} to decrease to 1.77 %. Compared to the COV_{Pmax} obtained at the − 2 °CA injection timing, it is thought that a better combustion situation can be achieved due to the fact that more time will be obtained for the formation of a homogeneous mixture in the cylinder by taking the injection start timing earlier, and as a result, a decrease in the COV_{Pmax} is considered. The most stable changes of P_{max} values for all the fuel types were obtained as COV_{Pmax} 0.88 % for FBDF, 0.75 % for E5B1 and 0.85 % for E15B3 in 10 % pilot fuel injection application.

Fig. 15 shows the effects of the engine parameters and the test fuels on COV_{MPRR}. It was observed that the rise in the alcohol fuel ratio under the same experiment conditions increased the COV_{MPRR} values. Compared with the main application, it was determined that the boost applications increased the COV changes in MPRR values for all the test fuels. The maximum COV_{MPRR} value was found to be 22.6 % in the use of E15B3, but the minimum COV_{MPRR} was calculated as 12.3 % in the 10 % pilot implementation with FBDF fuel. The reason for the lower COV_{MPRR} values in FBDF can be explained by the fact that it has the highest cetane number and viscosity value among the test fuels. It was determined that the COV_{MPRR} values were above 10 % in all the test conditions and in all the fuel types. In all test fuels, the approach of the SOI timing to the TDC caused a rise in COV_{MPRR}, while the advancing SOI from the TDC caused a decrease in COV_{MPRR}. It is thought that taken SOI timing earlier, a better combustion occurs in the cylinder since the fuels are mixed more homogeneously.

On the other hand, it was seen in the test results that the lowest COV values were obtained between 0.5 % and 0.92 % for CN values at all the fuel types. It was seen that the COV_{CN} values were generally below 1 % and a very stable change took place. In addition, the COV_{IMEP} values ranged from 0.5 % to 1 %, while COV_{Pmax} values were higher than COV_{IMEP} and ranged from 0.75 % to 2.3 %. In the COV_{MPRR} calculations, unstable values were seen between 12.3 % and 22.6 %.

3.9. FEA analysis

In the structural analysis studies, the result of the analysis in which 74.5 bar maximum cylinder gas pressure is applied to the piston head and the von Mises stress distribution are given in Fig. 16. It was observed that the stress distribution occurs similar to the literature and the

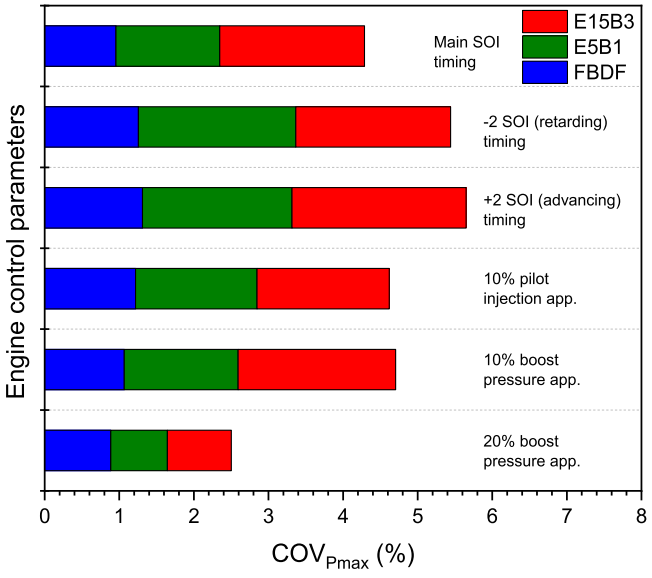

Fig. 14. Change in COV_{Pmax} under different engine parameters.

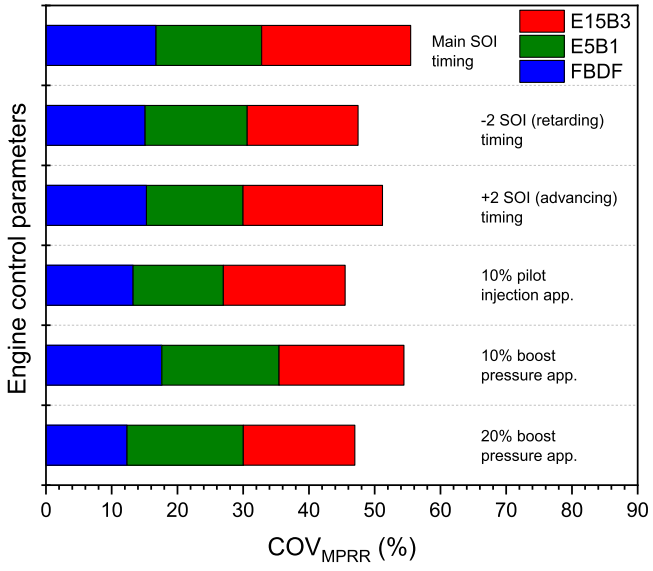

Fig. 15. Change in COV_{MPRR} under different engine parameters.

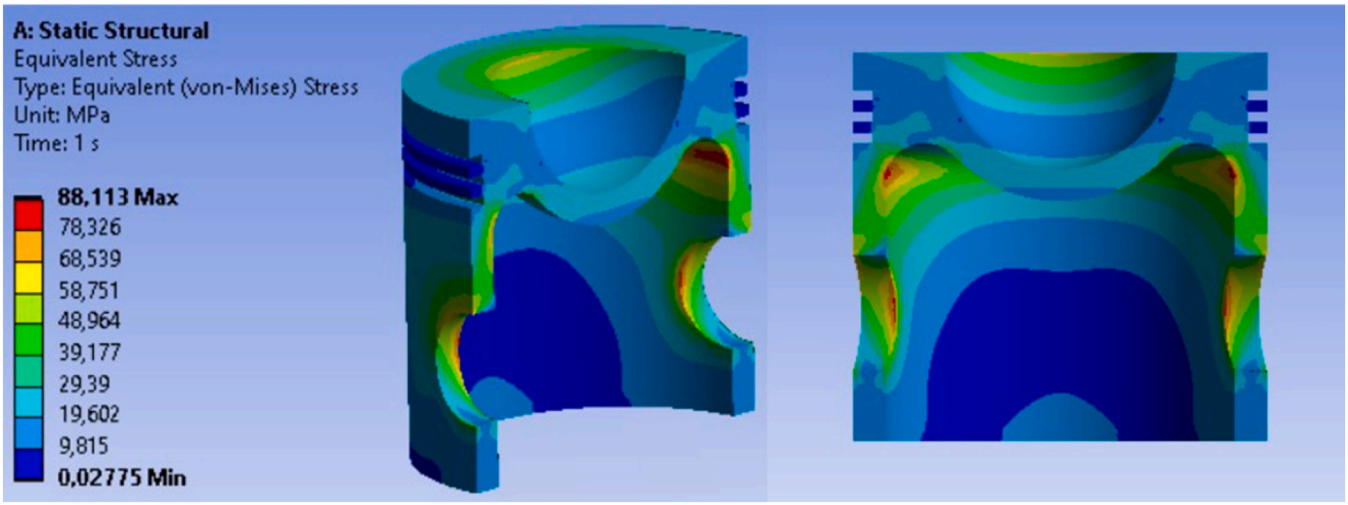

Fig. 16. Stress distribution of the aluminum piston.

maximum stress occurs in the piston pin holes (Dhinesh et al., 2018; Vedharaj et al., 2014). The graph showing the applied pressure and the corresponding stress values according to the motor control parameters is presented in Fig. 17. When these curves were examined, it was seen that the von Mises stress value increased and decreased proportionally with the pressure. The highest strain was obtained with E5B1 fuel at + 2 SOI timing engine control parameter. However, it was observed that the Al piston material, which has a yield strength of 290 MPa even at the maximum tensile value of 99.495 MPa, is approximately 2.9 times safe against permanent deformation (Manuel et al., 2012).

4. Conclusion

In this study, the impact of main engine parameters (injection timing, pilot injection and boost pressure) and cycle-to-cycle analysis on combustion and exhaust emissions in a single-cylinder compression ignition engine with common rail fuel injection system was carried out using triple mixture fuels (ethanol-2butanol-diesel) at the constant engine speed of 1400 rpm and 50 % of the gas pedal position.

- Use of 2-butanol for ethanol/diesel mixtures allowed the mixed fuels to keep homogeneous for a longer time. In future studies, 2-butanol can be considered as a solvent for ethanol/diesel mixtures.

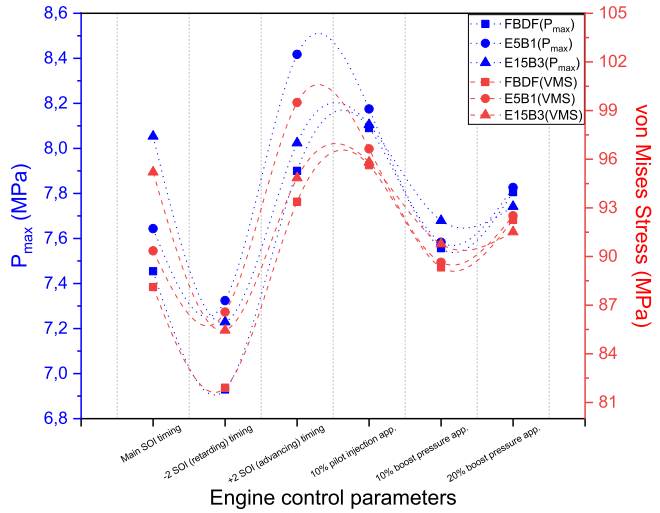

Fig. 17. Change in von Mises Stress under different engine parameters.

- Maximum IMEP for all fuel types was obtained as 7.8 bar for FBDF, 7.57 bar for E5B1 and 7.3 bar for E15B3 as a result of pilot injection implementation. The decrease in the ratio of the FBDF in blend fuels caused up to 5 % reduction in the IMEP values for all tested engine parameter.
- With the rise in the alcohol content in the mixtures, an improvement of up to 5 % was detected in the maximum cylinder gas pressure. The highest P_{max} was obtained as 84.1 bar in the application of + 2 advanced injection start timing with E5B1 fuel.
- CN and MPRR generally showed the similar trend. Compared to FBDF, the use of blended fuels resulted in a rise in CN and MPRR in other applications except pilot injection. Maximum CN and MPRR values were obtained in E15B3 fuel at 92.87 dB and 13 bar, respectively.
- Compared to the FBDF fuel, as with the increase in the alcohol rate in the blend fuels, the ID lengthened by approximately 20 %, while the MFB50 and the DOC times were shortened by more than 20 % and 15 %, respectively.
- For all fuel types, pilot injection implementation and + 2 advanced injection start timing resulted in increases in NO_X and CO_2 emissions of more than 20 % and more than 10 %, respectively. Maximum CO_2 and NO_x emissions were 5.7 % and 670 ppm for FBDF, 5.5 % and 650 ppm for E5B1, 5.34 % and 632 ppm for E15B3, respectively, in the pilot injection application.
- It was seen that the rise in alcohol fuel ratio in the mixture causes an increase in COV. It was seen that the changes in the COV_{CN}, the COV_{IMEP} and the COV_{Pmax} values were stable and less than 3 % while the changes in the COV_{MPRR} values were not stable and were more than 10 % in all the fuel types.
- Maximum von Mises stress was obtained as 99.495 MPa at + 2 SOI timing application with E5B1 fuel. It was determined that the piston body is 2.9 times safe against plastic deformation under the maximum stress condition.

As it is known, the most critical challenges to be overcome in today's commercial diesel engines are combustion noise and NO_x emission. This study indicates that the fuel injection parameters and alcohol/diesel blends have significant effect on NO_x emission and combustion noise level in diesel engines. It can be said that NO_x emissions and combustion noise level will be reduced easily in commercial diesel engines using pilot injection application and alcohol/diesel mixtures. However, more extensive exhaust emission studies are needed for more active use of alcoholic fuels.

Declaration of Competing Interest

The authors declare that they have no known competing financial interests or personal relationships that could have appeared to influence the work reported in this paper.

Acknowledgments

This study was supported by Kocaeli University Scientific Research Unit with the project number 2018/062.

References

Altun, Ş., Fırat, M., Varol, Y., Okcu, M., 2023. Comparison of direct and port injection of methanol in a RCCI engine using diesel and biodiesel as high reactivity fuels. Process Saf. Environ. Prot. 174, 681–693. https://doi.org/10.1016/j.psep.2023.04.033.

Amaral, B.S., Novaes, F.J.M., Ramos, M., da, C.K.V., Neto, F.R., de, A., Gioda, A., 2016. Comparative profile of pollutants generated by a stationary engine fueled with diesel, biodiesel, and ethanol. J. Aerosol Sci. 100, 155–163. https://doi.org/10.1016/j.jaerosci.2016.07.009.

Ashok, B., Denis Ashok, S., Ramesh Kumar, C., 2015. LPG diesel dual fuel engine - a critical review. Alex. Eng. J. 54, 105–126. https://doi.org/10.1016/j.aej.2015.03.002.

Biswas, S., Kakati, D., Chakraborti, P., Banerjee, R., 2021. Assessing the potential of ethanol in the transition of biodiesel combustion to RCCI regimes under varying injection phasing strategies: a performance-emission-stability and tribological perspective. Fuel 304. https://doi.org/10.1016/j.fuel.2021.121346.

Breuer, J.L., Samsun, R.C., Stolten, D., Peters, R., 2021. How to reduce the greenhouse gas emissions and air pollution caused by light and heavy duty vehicles with battery-electric, fuel cell-electric and catenary trucks. Environ. Int 152. https://doi.org/10.1016/j.envint.2021.106474.

Bunting, B.G., Wildman, C.B., Szybtst, J.P., Lewis, S., Storey, J., 2007. Fuel chemistry and cetane effects on diesel homogeneous charge compression ignition performance, combustion, and emissions. Int. J. Engine Res. https://doi.org/10.1243/14680874JER01306.

Chen, G., Shen, Y., Zhang, Q., Yao, M., Zheng, Z., Liu, H., 2013. Experimental study on combustion and emission characteristics of a diesel engine fueled with 2,5-dimethylfuran-diesel, n-butanol-diesel and gasoline-diesel blends. Energy 54. https://doi.org/10.1016/j.energy.2013.02.069.

Chickos, J.S., Acree, W.E., 2003. Enthalpies of vaporization of organic and organometallic compounds, 1880-2002. J. Phys. Chem. Ref. Data. https://doi.org/10.1063/1.1529214.

Cova-Bonillo, A., Patiño-Camino, R., Hernández, J.J., Lapuerta, M., 2022. Autoignition of ethanol-diesel blends: is it worth dehydrating ethanol. Fuel 317. https://doi.org/10.1016/j.fuel.2022.123523.

d'Ambrosio, S., Ferrari, A., Iemmolo, D., Mittica, A., 2019. Dependence of combustion noise on engine calibration parameters by means of the response surface methodology in passenger car diesel engines. Appl. Therm. Eng. 163. https://doi.org/10.1016/j.applthermaleng.2019.114209.

d'Ambrosio, S., Ferrari, A., Jin, Z., 2022. Time-frequency analysis application to the evaluation of instantaneous combustion noise. Fuel 312. https://doi.org/10.1016/j.fuel.2021.122655.

De Poures, M.V., Dillikannan, D., Kaliyaperumal, G., Thanikodi, S., Ağbulut, Ü., Hoang, A.T., Mahmoud, Z., Shaik, S., Saleel, C.A., Afzal, A., 2023. Collective influence and optimization of 1-hexanol, fuel injection timing, and EGR to control toxic emissions from a light-duty agricultural diesel engine fueled with diesel/waste cooking oil methyl ester blends. Process Saf. Environ. Prot. 172, 738–752. https://doi.org/10.1016/j.psep.2023.02.054.

Dharma, S., Ong, H.C., Masjuki, H.H., Sebayang, A.H., Silitonga, A.S., 2016. An overview of engine durability and compatibility using biodiesel–bioethanol–diesel blends in compression-ignition engines. Energy Convers. Manag. https://doi.org/10.1016/j.enconman.2016.08.072.

Dhinesh, B., Maria Ambrose Raj, Y., Kalaiselvan, C., KrishnaMoorthy, R., 2018. A numerical and experimental assessment of a coated diesel engine powered by high-performance nano biofuel. Energy Convers. Manag. 171, 815–824. https://doi.org/10.1016/j.enconman.2018.06.039.

Duan, X., Xu, Z., Deng, B., Liu, J., 2021. Effects of injection timing and EGR on combustion and emissions characteristics of the diesel engine fuelled with acetone–butanol–ethanol/diesel blend fuels. Energy, 121069. https://doi.org/10.1016/j.energy.2021.121069.

EL-Seesy, A.I., Kayatas, Z., Takayama, R., He, Z., Kandasamy, S., Kosaka, H., 2020. Combustion and emission characteristics of RCEM and common rail diesel engine working with diesel fuel and ethanol/hydrous ethanol injected in the intake and exhaust port: assessment and comparison. Energy Convers. Manag. 205. https://doi.org/10.1016/j.enconman.2019.112453.

Friedrich, P., Ortner, R., 2012. Sound Level of Motor Vehicles, Directorate General for Internal Policies.

Gad, M.S., He, Z., El-Shafay, A.S., El-Seesy, A.I., 2021. Combustion characteristics of a diesel engine running with Mandarin essential oil -diesel mixtures and propanol additive under different exhaust gas recirculation: experimental investigation and numerical simulation. Case Stud. Therm. Eng. 26. https://doi.org/10.1016/j.csite.2021.101100.

Ge, J.C., Wu, G., Choi, N.J., 2022. Comparative study of pilot–main injection timings and diesel/ethanol binary blends on combustion, emission and microstructure of particles emitted from diesel engines. Fuel 313. https://doi.org/10.1016/j.fuel.2021.122658.

Gren, L., Malmborg, V.B., Falk, J., Markula, L., Novakovic, M., Shamun, S., Eriksson, A. C., Kristensen, T.B., Svenningsson, B., Tunér, M., Karjalainen, P., Pagels, J., 2021. Effects of renewable fuel and exhaust aftertreatment on primary and secondary emissions from a modern heavy-duty diesel engine. J. Aerosol Sci. 156. https://doi.org/10.1016/j.jaerosci.2021.105781.

Han, J., He, W., Somers, L.M.T., 2020. Experimental investigation of performance and emissions of ethanol and n-butanol fuel blends in a heavy-duty diesel engine. Front. Mech. Eng. 6. https://doi.org/10.3389/fmech.2020.00026.

Hansen, A.C., Zhang, Q., Lyne, P.W.L., 2005. Ethanol-diesel fuel blends - a review. Bioresour. Technol. 96, 277–285. https://doi.org/10.1016/j.biortech.2004.04.007.

Huang, J., Wang, Y., Li, S., Roskilly, A.P., Yu, H., Li, H., 2009. Experimental investigation on the performance and emissions of a diesel engine fuelled with ethanol-diesel blends. Appl. Therm. Eng. 29. https://doi.org/10.1016/j.applthermaleng.2008.12.016.

Jin, C., Pang, X., Zhang, X., Wu, S., Ma, M., Xiang, Y., Ma, J., Ji, J., Wang, G., Liu, H., 2019. Effects of C3–C5 alcohols on solubility of alcohols/diesel blends. Fuel 236. https://doi.org/10.1016/j.fuel.2018.08.129.

Kim, H.Y., Ge, J.C., Choi, N.J., 2020. Effects of ethanol-diesel on the combustion and emissions from a diesel engine at a low idle speed. Appl. Sci. 10, 1–15. https://doi.org/10.3390/APP10124153.

Koutsakis, G., Ghandhi, J.B., 2022. Optimization of thermal barrier coating performance and durability over a drive cycle. Int. J. Engine Res. https://doi.org/10.1177/14680874221089072.

Kumar, N., Koul, R., Singh, R.C., 2022. Comparative analysis of ternary blends of renewable diesel, diesel and ethanol with diesel. Sustain. Energy Technol. Assess. 50, 101828 https://doi.org/10.1016/j.seta.2021.101828.

Lapuerta, M., Armas, O., García-Contreras, R., 2007. Stability of diesel-bioethanol blends for use in diesel engines. Fuel 86. https://doi.org/10.1016/j.fuel.2006.11.042.

Lapuerta, M., García-Contreras, R., Campos-Fernández, J., Dorado, M.P., 2010. Stability, lubricity, viscosity, and cold-flow properties of alcohol-diesel blends. Energy Fuels 24. https://doi.org/10.1021/ef100498u.

Leach, F., Kalghatgi, G., Stone, R., Miles, P., 2020. The scope for improving the efficiency and environmental impact of internal combustion engines. Transp. Eng. https://doi.org/10.1016/j.treng.2020.100005.

Lee, S., Kim, T.Y., 2015. Feasibility study of using wood pyrolysis oil-ethanol blended fuel with diesel pilot injection in a diesel engine. Fuel 162. https://doi.org/10.1016/j.fuel.2015.08.049.

Li, J., Zhang, Z., Ye, Y., Li, W., Yuan, T., Wang, H., Li, Y., Tan, D., Zhang, C., 2022. Effects of different injection timing on the performance, combustion and emission characteristics of diesel/ethanol/n-butanol blended diesel engine based on multi-objective optimization theory. Energy 260, 125056. https://doi.org/10.1016/j.energy.2022.125056.

Liu, J., Dumitrescu, C.E., 2019. Single and double Wiebe function combustion model for a heavy-duty diesel engine retrofitted to natural-gas spark-ignition. Appl. Energy 248. https://doi.org/10.1016/j.apenergy.2019.04.098.

Liu, J., Wu, P., Ji, Q., Sun, P., Wang, P., Meng, Z., Ma, H., 2022. Experimental study on effects of pilot injection strategy on combustion and emission characteristics of diesel/methanol dual-fuel engine under low load. Energy 247. https://doi.org/10.1016/j.energy.2022.123464.

Liu, S., Shen, L., Bi, Y., Lei, J., 2014. Effects of altitude and fuel oxygen content on the performance of a high pressure common rail diesel engine. Fuel 118. https://doi.org/10.1016/j.fuel.2013.10.007.

Manuel, J., Aguilar, A., Arroyo, R.L., Cruz, J.M., Celaya, M., Guanajuato, M., 2012. Study of the thermal-structural behavior of a piston diesel with gallery through finite element method.

Mendes Guedes, A.D., Leal Braga, S., Pradelle, F., 2018. Performance and combustion characteristics of a compression ignition engine running on diesel-biodiesel-ethanol (DBE) blends – Part 2: Optimization of injection timing. Fuel 225, 174–183. https://doi.org/10.1016/j.fuel.2018.02.120.

Nabi, M.N., Akhter, M.S., Shahadat, M.M.Z., 2006. Improvement of engine emissions with conventional diesel fuel and diesel-biodiesel blends. Bioresour. Technol. 97, 372–378. https://doi.org/10.1016/j.biortech.2005.03.013.

Nanthagopal, K., Kishna, R.S., Atabani, A.E., Al-Muhtaseb, A.H., Kumar, G., Ashok, B., 2020. A compressive review on the effects of alcohols and nanoparticles as an oxygenated enhancer in compression ignition engine. Energy Convers. Manag. https://doi.org/10.1016/j.enconman.2019.112244.

Ning, L., Duan, Q., Chen, Z., Kou, H., Liu, B., Yang, B., Zeng, K., 2020. A comparative study on the combustion and emissions of a non-road common rail diesel engine fueled with primary alcohol fuels (methanol, ethanol, and n-butanol)/diesel dual fuel. Fuel 266. https://doi.org/10.1016/j.fuel.2020.117034.

Panoutsou, C., Germer, S., Karka, P., Papadokostantakis, S., Kroyan, Y., Wojcieszyk, M., Maniatis, K., Marchand, P., Landalv, I., 2021. Advanced biofuels to decarbonise European transport by 2030: Markets, challenges, and policies that impact their successful market uptake. Energy Strategy Rev. 34. https://doi.org/10.1016/j.esr.2021.100633.

Paque, G., 2003. The EU environmental noise policy: an integrated approach. Acta Acustica 89.

Park, S.H., Youn, I.M., Lee, C.S., 2010. Influence of two-stage injection and exhaust gas recirculation on the emissions reduction in an ethanol-blended diesel-fueled four-cylinder diesel engine. Fuel Process. Technol. 91. https://doi.org/10.1016/j.fuproc.2010.07.016.

Reyes, Y., Aranda, D.A.G., Santander, L.A.M., Cavado, A., Belchior, C.R.P., 2009. Action principles of cosolvent additives in ethanol - Diesel blends: Stability studies. Energy Fuels 23. https://doi.org/10.1021/ef8010492.

Saiteja, P., Ashok, B., 2021. A critical insight review on homogeneous charge compression ignition engine characteristics powered by biofuels. Fuel 285. https://doi.org/10.1016/j.fuel.2020.119202.

Sarathy, S.M., Oßwald, P., Hansen, N., Kohse-Höinghaus, K., 2014. Alcohol combustion chemistry. Prog. Energy Combust. Sci. 44, 40–102. https://doi.org/10.1016/j.pecs.2014.04.003.

Satgé De Caro, P., Mouloungui, Z., Vaitilingom, G., Berge, J.C., 2001. Interest of combining an additive with diesel-ethanol blends for use in diesel engines. Fuel 80. https://doi.org/10.1016/S0016-2361(00)00117-4.

Shen, M., Tuner, M., Johansson, B., Cannella, W., 2013. In: Technical Papers, S.A.E. (Ed.), Effects of EGR and Intake Pressure on PPC of Conventional Diesel, Gasoline and Ethanol in A Heavy Duty Diesel Engine. https://doi.org/10.4271/2013-01-2702.

Singh, A., Tsolas, N., 2023. Sooting tendency of isopropanol-butanol-ethanol (IBE)/diesel surrogate blends in laminar diffusion flames. Combust. Flame 250, 112630. https://doi.org/10.1016/J.COMBUSTFLAME.2023.112630.

Turkcan, A., 2020. The effects of different types of biodiesels and biodiesel-bioethanol-diesel blends on the cyclic variations and correlation coefficient. Fuel 261. https://doi.org/10.1016/j.fuel.2019.116453.

Vedharaj, S., Vallinayagam, R., Yang, W.M., Chou, S.K., Chua, K.J.E., Lee, P.S., 2014. Experimental and finite element analysis of a coated diesel engine fueled by cashew nut shell liquid biodiesel. Exp. Therm. Fluid Sci. 53, 259–268. https://doi.org/10.1016/j.expthermflusci.2013.12.018.

Wang, S., Liang, Y., Zhu, J., Raza, M., Li, J., Yu, L., Qian, Y., Lu, X., 2021. Experimental and modeling study of the autoignition for diesel and n-alcohol blends from ethanol to n-pentanol in shock tube and rapid compression machine. Combust. Flame 227, 296–308. https://doi.org/10.1016/j.combustflame.2021.01.019.

Wang, Z., Liu, H., Song, T., Qi, Y., He, X., Shuai, S., Wang, J., 2015. Relationship between super-knock and pre-ignition. Int. J. Engine Res. 16. https://doi.org/10.1177/1468087414530388.

Xin, Q., 2013. Durability and reliability in diesel engine system design, in: Diesel Engine System Design. ⟨https://doi.org/10.1533/9780857090836.1.113⟩.

Xuan, T., Sun, Z., EL-Seesy, A.I., Mi, Y., Zhong, W., He, Z., Wang, Q., Sun, J., El-Batsh, H. M., Cao, J., 2021. An optical study on spray and combustion characteristics of ternary hydrogenated catalytic biodiesel/methanol/n-octanol blends; part II: liquid length and in-flame soot. Energy 227. https://doi.org/10.1016/j.energy.2021.120543.

Yilmaz, N., Davis, S.M., 2022. Diesel blends with high concentrations of biodiesel and n-butanol: effects on regulated pollutants and polycyclic aromatic hydrocarbons. Process Saf. Environ. Prot. 166, 430–439. https://doi.org/10.1016/j.psep.2022.08.041.

Zhang, Z., Tian, J., Xie, G., Li, J., Xu, W., Jiang, F., Huang, Y., Tan, D., 2022. Investigation on the combustion and emission characteristics of diesel engine fueled with diesel/methanol/n-butanol blends. Fuel 314. https://doi.org/10.1016/j.fuel.2021.123088.

Zhao, W., Yan, J., Gao, S., Lee, T.H., Li, X., 2022. The combustion and emission characteristics of a common-rail diesel engine fueled with diesel, propanol, and pentanol blends under low intake pressures. Fuel 307. https://doi.org/10.1016/j.fuel.2021.121692.